Inorganic Chemistry

Article

pubs.acs.org/IC

Synthetic and Coordination Chemistry of the Heavier Trivalent Technetium Binary Halides: Uncovering Technetium Triiodide

Erik V. Johnstone,*[,†] Frederic Poineau,[†] Jenna Starkey,[‡] Thomas Hartmann,[§] Paul M. Forster,[†] Longzhou Ma,[§] Jeremy Hilgar,[†] Efrain E. Rodriguez,[∥] Romina Farmand,[†] Kenneth R. Czerwinski,[†] and Alfred P. Sattelberger[†,⊥]

[†]Department of Chemistry, University of Nevada—Las Vegas, Las Vegas, Nevada 89154, United States

[‡]Department of Chemistry, Virginia Wesleyan College, Norfolk, Virginia 23502, United States

[§]Harry Reid Center for Environmental Studies, Las Vegas, Nevada 89154, United States

[∥]Department of Chemistry, University of Maryland, College Park, Maryland 20742, United States

[⊥]Energy Engineering and Systems Analysis Directorate, Argonne National Laboratory, Argonne, Illinois 60439, United States

Supporting Information

ABSTRACT: Technetium tribromide and triiodide were obtained from the reaction of the quadruply Tc−Tc-bonded dimer $Tc_2(O_2CCH_3)_4Cl_2$ with flowing HX(g) (X = Br, I) at elevated temperatures. At 150 and 300 °C, the reaction with HBr(g) yields $TcBr_3$ crystallizing with the TiI_3 structure type. The analogous reactions with flowing HI(g) yield TcI_3, the first technetium binary iodide to be reported. Powder X-ray diffraction (PXRD) measurements show the compound to be amorphous at 150 °C and semicrystalline at 300 °C. X-ray absorption fine structure spectroscopy indicates TcI_3 to consist of face-sharing TcI_6 octahedra. Reactions of technetium metal with elemental iodine in a sealed Pyrex ampules in the temperature range 250−400 °C were performed. At 250 °C, no reaction occurred, while the reaction at 400 °C yielded a product whose PXRD pattern matches the one of TcI_3 obtained from the reaction of $Tc_2(O_2CCH_3)_4Cl_2$ and flowing HI(g). The thermal stability of $TcBr_3$ and TcI_3 was investigated in Pyrex and/or quartz ampules at 450 °C under vacuum. Technetium tribromide decomposes to $Na\{[Tc_6Br_{12}]_2Br\}$ in a Pyrex ampule and to technetium metal in a quartz ampule; technetium triiodide decomposes to technetium metal in a Pyrex ampule.

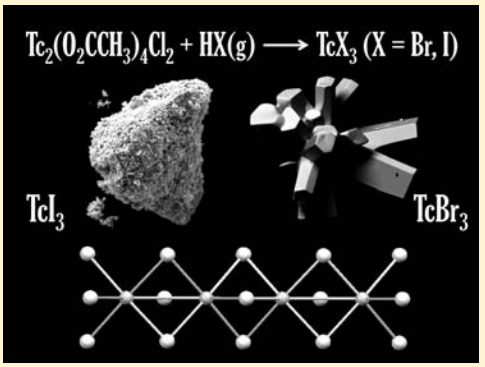

INTRODUCTION

In the past 5 years, the chemistry of technetium binary halides has experienced rapid development and five new phases were reported, which brings the total number of known technetium binary halides to eight. These include two fluorides (TcF_6 and TcF_5), four chlorides ($TcCl_4$, α/β-$TcCl_3$, and $TcCl_2$), and two bromides ($TcBr_4$ and $TcBr_3$).[1−4] Trivalent technetium halides have a rich chemistry, and three phases have been reported: $TcBr_3$, α-$TcCl_3$, and β-$TcCl_3$.[2−4] These phases exhibit various dimensionalities and consist of either clusters or infinite chains and layers of TcX_6 (X = Cl, Br) octahedra (Chart 1).

Because technetium is the lighter congener of rhenium, it often demonstrates chemically similar behavior. This is observed for the homologous reaction of $Tc_2(O_2CCH_3)_4Cl_2$ with flowing HCl(g) at 300 °C, which yields α-$TcCl_3$ with the $ReCl_3$ structure type (Chart 1A).[3,5] α-$TcCl_3$ has also been synthesized from decomposition of $TcCl_4$ under vacuum at 450 °C and from the thermal treatment of β-$TcCl_3$ at 280 °C under vacuum.[4,6] Unlike α-$TcCl_3$, β-$TcCl_3$ exhibits structural similarities to the ruthenium and molybdenum analogues, crystallizing with the $AlCl_3$ structure type (Chart 1B).[4] This structural similarity with the ruthenium and molybdenum analogues is also observed for $TcBr_3$.

Technetium tribromide has been obtained congruently with $TcBr_4$ from stoichiometric reactions of the elements in sealed tubes at elevated temperatures. These reactions yield a $TcBr_3$ phase with the TiI_3 structure type consisting of extended chains of infinite-ordered face-sharing $TcBr_6$ octahedra (Chart 1C).[2] First-principles theoretical calculations predicted the existence of a second tribromide phase, Tc_3Br_9, which would be isostructural to α-$TcCl_3$ and Re_3Br_9.[7] A previous study mentioned that Tc_3Br_9 was obtained from bromination of $[Tc(CO)_3Br]_4$, but no crystallographic data were reported.[8] With regard to this information, the existence of Tc_3Cl_9, and the trend of the Re_3X_9 system (X = Cl, Br, I),[5] it was of interest to perform the reaction of $Tc_2(O_2CCH_3)_4Cl_2$ with flowing HBr(g) at elevated temperatures in an attempt to isolate Tc_3Br_9.

Interestingly, binary transition-metal iodides have been reported for all second- and third-row group IV−XI elements

Received: September 7, 2013
Published: December 2, 2013

   dx.doi.org/10.1021/ic402278c | Inorg. Chem. 2013, 52, 14309−14316

Chart 1. Ball-and-Stick Representations of the Structures Exhibited by Binary Technetium Trihalides: (a) α-$TcCl_3$, (b) β-$TcCl_3$, and (c) $TcBr_3$[a]

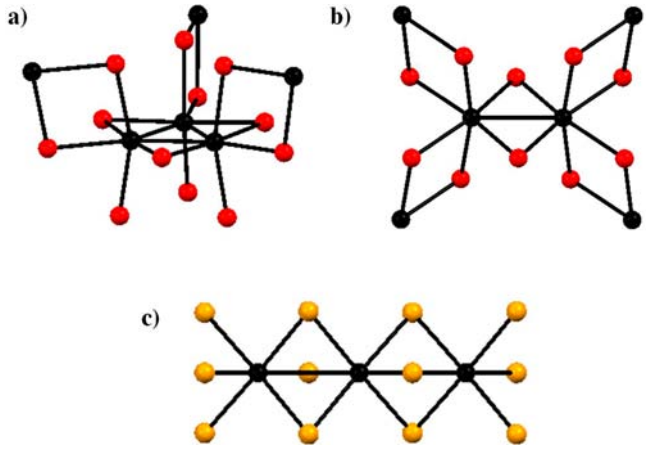

[a]Tc atoms are in black, Cl atoms are in red, and Br atoms are in orange.

with the exception of technetium.[1b,9] Binary transition-metal iodides can be obtained by either of two methods: (1) the reaction between flowing HI(g) and a multiply metal−metal-bonded acetate dimer or (2) the reaction between the elements in a sealed tube. To the best of our knowledge, neither of these reactions has been reported for technetium. Because technetium and iodine both have isotopes resulting from the fission of uranium fuel, i.e., ^{99}Tc and ^{129}I, it was also of interest to gain a better understanding of the chemical reactivity of technetium with iodine for potential nuclear fuel cycle applications.[10]

Thermal decomposition of binary transition-metal halides is a practical method for isolating low-valent phases.[11] For technetium, previous studies performed at 450 °C under vacuum have shown that $TcCl_4$ decomposes sequentially to α-$TcCl_3$ and $TcCl_2$, while $TcBr_4$ decomposes to $TcBr_3$ and $Na\{[Tc_6Br_{12}]_2Br\}$.[6,12]

In this paper, we report the reactions of $Tc_2(O_2CCH_3)_4Cl_2$ with flowing HX(g) (X = Br, I) at 150 and 300 °C and the reaction of technetium metal with iodine in sealed Pyrex ampules. The reaction products were characterized using powder X-ray diffraction (PXRD), energy-dispersive X-ray (EDX) spectroscopy, IR spectroscopy, and X-ray absorption fine structure spectroscopy (XAFS). The thermal properties of $TcBr_3$ and TcI_3 were studied under vacuum in sealed ampules at elevated temperature. Finally, the coordination and synthetic chemistry of the heavier technetium trihalides are discussed and compared to their molybdenum, ruthenium, and rhenium analogues.

EXPERIMENTAL SECTION

Caution! *Technetium-99 is a weak β-emitter (E_{max} = 292 keV). All manipulations were performed in a laboratory designed for handling radioactive materials using efficient HEPA-filtered fume hoods and Schlenk and glovebox techniques and following locally approved radiochemistry handling and monitoring procedures. Laboratory coats, disposable gloves, and protective eyewear were worn at all times.*

Synthesis. *Reagents.* Technetium metal and $Tc_2(O_2CCH_3)_4Cl_2$ were prepared according to the methods previously reported.[4,13] A lecture bottle of HBr(g), elemental iodine, and gold foil (0.1 mm thick, 99.99%) were purchased from Sigma-Aldrich and used as received. A lecture bottle of HI(g) was obtained from Matheson-Trigas.

Experimental Setup for Flowing Gas Reactions (Figure S1 in the Supporting Information, SI). A 50 cm long quartz tube fitted with Solv-Seal end joints and two gas inlets/outlets was used. The inlet was connected with Teflon tubing to a T-shaped stopcock controlling the flow of HX(g) (X = Br, I) or Ar(g), and the outlet was connected to a bubbler trap filled with concentrated H_2SO_4. The tube was placed in a Thermo Fisher Scientific Lindberg/Blue M Mini-Mite clamshell furnace with a 8-cm-long quartz boat containing $Tc_2(O_2CCH_3)_4Cl_2$ located directly above the thermocouple of the furnace. For each reaction, the tube was initially purged with flowing Ar(g) and the temperature was increased to 150 °C and held there for a minimum of 10 min. This was done to prevent the premature reaction of HX(g) with the compound, resulting in the release of acetic acid below its boiling point (117 °C).

Reaction of $Tc_2(O_2CCH_3)_4Cl_2$ with HBr(g) at 150 °C. $Tc_2(O_2CCH_3)_4Cl_2$ (65.6 mg, 0.13 mmol) was evenly dispersed in a quartz boat. The boat was placed in the middle of a quartz tube situated in the clamshell furnace. The tube was initially purged with Ar(g) for 15 min at room temperature; the temperature was then increased to 150 °C (10 °C/min) and held for 5 min. Using a T-shaped stopcock, the gas was switched to HBr(g), and an immediate color change from crimson to black-purple was observed. The compound was reacted for 1 h under flowing HBr(g) at 150 °C, after which the tube was cooled to room temperature under flowing HBr(g). After the reaction, the black $TcBr_3$ powder (86.5 mg, 0.26 mmol, yield = 98%) was placed in a Pyrex tube (L = 30 cm) and sealed (L = 18 cm) under vacuum (1 mTorr). The sealed tube was placed in a clamshell furnace, heated to 150 °C (10 °C/min), and held there for 24 h; a small amount of a black amorphous film sublimed to the cooler end of the tube, and the remaining powder was characterized by PXRD.

Reaction of $Tc_2(O_2CCH_3)_4Cl_2$ with HBr(g) at 300 °C. The reaction of $Tc_2(O_2CCH_3)_4Cl_2$ (67.8 mg, 0.13 mmol) with flowing HBr(g) at 300 °C was performed using the same method as that above. The apparatus was purged with Ar(g) for 15 min, and the temperature was increased (10 °C/min) to 150 °C and held for 5 min, after which the atmosphere was switched to HBr(g) and the temperature was then increased (10 °C/min) to 300 °C and held there for 1 h. After the reaction, 83.4 mg (0.25 mmol) of the black-purple $TcBr_3$ powder was recovered (95% yield). The powder was sealed in a Pyrex tube (L = 18 cm) under vacuum and heated in the furnace at 300 °C for 24 h; a dark film at the coolest portion of the tube was observed, and the remaining powder was analyzed by PXRD and IR spectroscopy.

Reaction of $Tc_2(O_2CCH_3)_4Cl_2$ with HI(g) at 150 °C. The reactions with HI(g) were performed in an experimental setup similar to the one used for the reaction with HBr(g). $Tc_2(O_2CCH_3)_4Cl_2$ (74.0 mg, 0.15 mmol) was evenly dispersed in a quartz boat lined with a 0.1-mm-thick gold foil.[14] The system was purged with Ar(g) for 15 min at room temperature; the temperature was then increased to 150 °C (10 °C/min) and held for 5 min, and the gas was immediately switched to HI(g). A rapid color change from crimson to deep black upon the introduction of HI(g) was observed. The compound was reacted for an additional 30 min under flowing HI(g) at 150 °C, after which the tube was cooled to room temperature under flowing HI(g). After the reaction, the black powder (111.7 mg) was analyzed by PXRD, ^{99}Tc elemental analysis, IR spectroscopy, and XAFS (vide infra). Following characterization, the remaining powder (47.7 mg) was placed in a gold envelope, which was introduced to a Pyrex tube and sealed under vacuum. The tube was sintered at 150 °C (10 °C/min) for 5 days. After the reaction, the black powder (36.4 mg) was characterized by PXRD and EDX spectroscopy.

Reaction of $Tc_2(O_2CCH_3)_4Cl_2$ with HI(g) at 300 °C. The same experimental procedure and apparatus as those of the reaction of HI(g) at 150 °C were used for the reaction at 300 °C. A weighted quantity of $Tc_2(O_2CCH_3)_4Cl_2$ (58.5 mg, 0.12 mmol) was evenly dispersed in a quartz boat lined with gold foil. The system was purged with Ar(g) for 15 min at room temperature; the temperature was then increased to 150 °C (10 °C/min) and held for 5 min under argon, and the gas was switched to HI(g). The system was then ramped (10 °C/

dx.doi.org/10.1021/ic402278c | Inorg. Chem. 2013, 52, 14309−14316

min) to 300 °C, held for 15 min at 300 °C, and cooled to room temperature under HI(g). The resulting black powder (95.4 mg) was analyzed by PXRD. A sample of the compound (59.0 mg) was placed in a gold capsule, sealed in a Pyrex ampule, and sintered at 300 °C. No single crystals were obtained after the reaction, and the sintered powder (50.4 mg) was analyzed by PXRD.

Reaction of Technetium Metal with Iodine. Technetium metal (36.8 mg, 0.37 mmol) was placed in a gold envelope in a Pyrex tube (L = 43 cm); the tube was connected to a Schlenk line and flamed under vacuum. After backfilling with Ar(g), the tube was removed from the Schlenk line and elemental iodine (188 mg, 0.74 mmol; Tc:I ~ 1:4) was quickly inserted into the tube. The tube was connected to the Schlenk line and flame-sealed (L = 18 cm) under vacuum. The tube was inserted into a clamshell furnace with the metal end of the sealed tube located in the center of the furnace. The temperature was increased to 400 °C (7.5 °C/min) and held at that temperature for 2 weeks. After cooling to room temperature, a black microcrystalline powder was observed at the cool end of the tube, but no single crystals were obtained. The black powder (78.9 mg, 30%) was analyzed by PXRD.

Decomposition of $TcBr_3$ in Pyrex. Technetium tribromide (32.0 mg, 94.5 mmol) was placed in a 30-cm-long Pyrex tube and flame-sealed at 18 cm under vacuum. The resulting tube was placed in a furnace with the solid at the center of the furnace and reacted at 450 °C for 24 h. After cooling to room temperature, the reaction yielded a dark crystalline powder, rail spike crystals adjacent to the powder, needle crystals at the cooler end of the tube, and a dark amorphous film at the end of the tube (Figure S2a in the SI). The rail spike and needle crystals were indexed by single-crystal X-ray diffraction (XRD), and the remaining solid was indexed by PXRD (Figure S6 in the SI).

Decomposition of $TcBr_3$ in Quartz. Technetium tribromide (32.2 mg, 95.1 mmol) was placed in a 30-cm-long quartz tube and sealed at 18 cm under vacuum. The tube was reacted using the same method as Pyrex decomposition for 24 h at 450 °C. After the reaction, the contents of the cooled tube included a grayish crystalline powder (10.6 mg), metallic purple needle crystals near the cooler portion of the tube, and a dark amorphous film at the end of the tube (Figure S2b in the SI). The single crystals were analyzed by single-crystal XRD, and the remaining powder was characterized by PXRD (Figure S7 in the SI).

Decomposition of TcI_3. Technetium triiodide (~24 mg, 0.05 mmol) was inserted into a gold foil capsule, placed in a 30 cm Pyrex tube, and flame-sealed under vacuum. The resulting tube (L = 18 cm) was placed in a clamshell furnace and reacted at 450 °C (10 °C/min) for 16 h. Once at temperature, the entire tube was bright purple from the release of I_2(g) from the sample. After cooling to room temperature, the tube contained a considerable amount of condensed iodine at the coolest portion but no crystalline technetium compounds. The resulting grayish-black powder (~8 mg, 0.08 mmol) was analyzed by PXRD (Figure S8 in the SI).

Characterization Methods. Single-crystal XRD data were collected on a Bruker Apex II system equipped with an Oxford nitrogen cryostream operating at 150 K. Crystals were mounted under Paratone on a glass fiber. Data processing was performed using the *Apex II* suite and an absorption correction performed with *SADABS*. Structure solution (direct methods) and refinement were carried out using *SHELX97*.[15]

PXRD patterns were obtained using a Bruker D8 advanced diffractometer employing Cu Kα_1 X-rays from 10 to 120° (2θ) with a step size of 0.008° (2θ) and 0.65 s/step. The PXRD patterns were quantified by Rietveld analysis using *Topas 4.0* software. The samples (~10–20 mg) were ground in an agate mortar and dispersed on a low-background silicon disk sample holder, covered with a radiological containment dome, and placed in the instrument for measurement.

XAFS. The XAFS measurements were performed at the Argonne National Laboratory Advanced Photon Source at the BESSRC-CAT 12 BM-B station. Technetium triiodide obtained from the reaction at 150 °C and Cs_2TcI_6 were diluted (3% in mass) in boron nitride. The samples were placed in a cavity of a Teflon sample holder and covered with a Kapton film. The XAFS spectra were recorded at the Tc K-edge (21044 eV) in transmission mode at room temperature. A double crystal of silicon [1 1 1] was used as a monochromator. The energy was calibrated using a molybdenum foil. A total of 10 scans were recorded in the k range 0–16 Å^{-1} and averaged. The extended XAFS (EXAFS) spectra were extracted using *Athena* software, and data analysis was performed using *Winxas*.[16] For the fitting procedure, the amplitude and phase shift functions were calculated by *FEFF 8.2*.[17] Input files were generated by *Atoms*.[18] Adjustments of the k^3-weighted EXAFS spectra were under the constraints S_0^2 = 0.9.

Other Techniques. Scanning electron microscopy (SEM) imaging and EDX measurements were performed on a JEOL model JSM-5610 scanning electron microscope equipped with secondary-electron and backscattered-electron detectors. Attenuated total reflectance Fourier transform infrared (ATR-FT-IR) spectra of the reacted powders were obtained on a Varian Excalibur spectrometer using a KBr beam splitter and an integrated Durasampler diamond ATR. ^{99}Tc concentrations were determined by liquid scintillation counting (LSC) using a Packard 2500 scintillation analyzer. The scintillation cocktail was ULTIMA GOLD ABTM (Packard).

RESULTS

A. Technetium Tribromide. *Characterization.* The powder patterns of the reaction products at 150 and 300 °C with HBr(g) are shown in Figure 1. Rietveld analyses of the

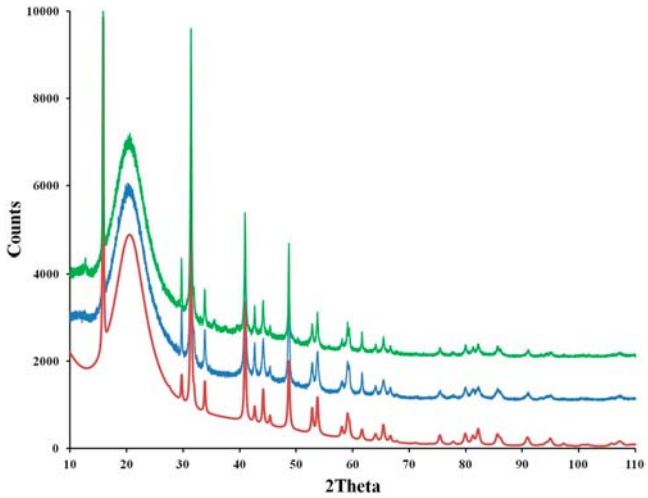

Figure 1. PXRD of products from the reaction of $Tc_2(O_2CCH_3)_4Cl_2$ with HBr(g) at 150 °C (green) and 300 °C (blue) and the calculated (red) pattern of $TcBr_3$. The amorphous hump from 2θ = 20 to 30° is due to a radiological containment dome.

powder patterns at both temperatures were fit as $TcBr_3$ with the TiI_3 structure type. Technetium tribromide obtained from the reaction of $Tc_2(O_2CCH_3)_4Cl_2$ with flowing HBr(g) at 150 and 300 °C [*Pnmmz*; a = 6.4806(3) Å, b = 11.2254(8) Å, c = 6.0206(3) Å and a = 6.4826(2) Å, b = 11.2296(7) Å, c = 6.0207(8) Å, respectively] is isostructural to $TcBr_3$ [*Pnmmz*; a = 6.3873(11) Å, b = 11.0618(18) Å, c = 5.9755(10) Å] obtained from reaction of the elements in a sealed tube and consists of infinite chains of face-sharing $TcBr_6$ octahedra. The weak peak at 2θ = 12.65 (d = 7.31) in the pattern of the product at 150 °C is attributed to an impurity of unreacted $Tc_2(O_2CCH_3)_4Cl_2$. The IR spectrum (Figure S9 in the SI) of the product obtained at 150 °C exhibits weak stretching modes (~1043 and 1022 cm^{-1}) from $Tc_2(O_2CCH_3)_4Cl_2$, while the product at 300 °C exhibits no stretching modes in this region, which indicates that the reaction went to completion. The elemental composition of the material obtained at 300 °C was

dx.doi.org/10.1021/ic402278c | *Inorg. Chem.* 2013, 52, 14309–14316

determined by EDX showing Tc L_α and Br L_α lines, confirming a binary technetium bromide (Figure S4 in the SI). The stoichiometry was determined to be 1:3.1(1) Tc/Br, confirming the presence of the tribromide.

Thermal Stability. The thermal behavior of $TcBr_3$, obtained from the reaction of $Tc_2(O_2CCH_3)_4Cl_2$ with flowing HBr(g) at 300 °C, was investigated in sealed Pyrex and quartz ampules under vacuum at 450 °C. Decomposition of $TcBr_3$ in the Pyrex ampule yielded results similar to decomposition of $TcBr_4$; the rail spike crystals sublimed adjacent to the powder and the needle crystals at the end of the tube were identified by single-crystal XRD to be $Na\{[Tc_6Br_{12}]_2Br\}$ and $TcBr_3$, respectively. In contrast, the reaction in quartz ampule resulted in $TcBr_3$ and technetium metal (Figure S7 in the SI).

B. Technetium Triiodide. *Characterization.* The product obtained from the reaction of $Tc_2(O_2CCH_3)_4Cl_2$ with flowing HI(g) at 150 °C was characterized by ^{99}Tc elemental analysis, EDX and IR spectroscopies, XAFS, and PXRD.

For ^{99}Tc elemental analysis, an aliquot (16.7 mg) of the solid was suspended in 10 mL of concentrated $HClO_4$. After 10 days, the solid had dissolved, the Tc concentration was determined by LSC, and the technetium content was consistent with the stoichiometry $TcI_{2.97(6)}$. The IR spectrum (Figure S9 in the SI) of TcI_3 shows the absence of stretching modes from 4000 to 500 cm^{-1}, confirming completion of the transformation of $Tc_2(O_2CCH_3)_4Cl_2$ to TcI_3. PXRD indicates the compound to be X-ray amorphous, and TcI_3 was characterized by XAFS.

XAFS has proven to be an efficient technique for the characterization of technetium complexes; complementary X-ray absorption near-edge structure (XANES) spectra can give information about the oxidation state of the absorbing atoms,[20] while the EXAFS spectrum contains information on the chemical environment around the absorbing atoms.[21,13] Recently, XAFS has been used to characterize the reaction of $Tc_2(O_2CCH_3)_4Cl_2$ with HCl(g) at 300 °C, and the results were consistent with the presence of the Tc_3Cl_9 cluster.[22] In order to determine whether TcI_3 exhibits ReI_3, $TcBr_3$, or some other structure, the compound was analyzed by XAFS.

The XANES spectrum of TcI_3 was recorded (Figure 2), background-subtracted, and normalized and the Tc K-edge

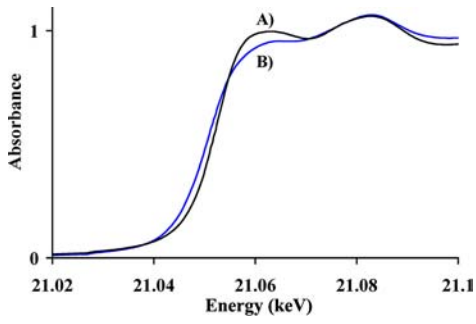

Figure 2. Normalized Tc K-edge XANES spectra of Cs_2TcI_6 (A in black) and TcI_3 (B in blue).

position determined using the first-derivative method. The position of the Tc K-edge of TcI_3 (21050.8 eV) is lower than the one of Cs_2TcI_6 (21053.0 eV) and similar to the ones of α-$TcCl_3$ (21051.0 eV) and β-$TcCl_3$ (21050.5 eV); these results are consistent the presence of Tc^{3+} atoms in TcI_3.[23]

The extracted EXAFS spectrum was k^3-weighted and the Fourier transform performed in the k range 2−14.5 $Å^{-1}$. Two different adjustments were performed considering the structure of a Tc_3I_9 cluster that exhibits the Tc_3Cl_9 structure and the structure of $TcBr_3$.[24,25] For the adjustment modeling the structure of ReI_3, the scattering functions were calculated in a Tc_3I_9 cluster with the Tc_3^{9+} triangular geometry (Figure 3a).

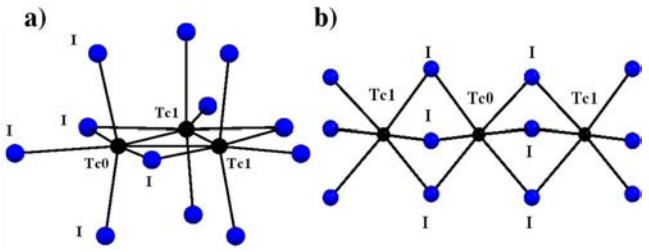

Figure 3. Ball-and-stick representations of the clusters used for EXAFS calculations: (a) cluster with the ReI_3 structure type; (b) cluster with the $TcBr_3$ structure type. Tc and I atoms are in black and blue, respectively. Tc0 represents the absorbing atom.

For the adjustment modeling the structure of $TcBr_3$, the scattering functions were calculated for a linear TcI_3 chain formed from face-sharing TcI_6 octahedron (Figure 3b). For the adjustments, the numbers of atoms were fixed at those of the clusters; ΔE_0 was constrained to be the same value for each wave; all of the other parameters were allowed to vary.

The best adjustment was obtained by modeling the structure of $TcBr_3$ (Figure 4); further details of the adjustment of the EXAFS spectra of TcI_3 based on the structure of $TcBr_3$ are presented in the SI (Figure S10). Adjustment modeling the structure of ReI_3 does not provide a suitable fit of the EXAFS spectra of TcI_3 and resulted in high value of the reduced χ^2 (Figure S10 in the SI).

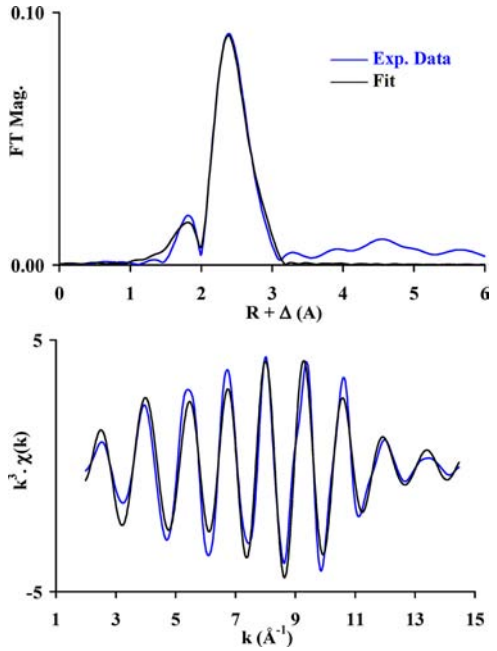

Figure 4. Fits of the experimental k^3-weighted EXAFS spectra (bottom) and Fourier transform of k^3-weighted EXAFS spectra (top) for the compound obtained from the reaction of $Tc_2(O_2CCH_3)_4Cl_2$ with HI(g) at 150 °C. Adjustment was performed between k = 2 and 14.5 $Å^{-1}$ considering the structure of $TcBr_3$. Experimental data are in blue, and the fits are in black.

dx.doi.org/10.1021/ic402278c | *Inorg. Chem.* 2013, 52, 14309−14316

The structural parameters (Table 1) found by EXAFS in TcI_3 show the presence of two Tc atoms at 3.10(3) Å and six I atoms at 2.67(3) Å. This data and the Tc0−Tc1 separation are consistent with the presence of face-sharing TcI_6 octahedra with the $TcBr_3$ structure type.[25]

Table 1. Structural Parameters Obtained by Adjustment of the k^3-Weighted EXAFS Spectra of the Compound Obtained from the Reaction of $Tc_2(O_2CCH_3)_4Cl_2$ with HI(g) at 150 °C (Adjustment between k = 2 and 14.5 Å^{-1} Considering the Structure of $TcBr_3$; ΔE_0 (eV) = −4.09 eV; Reduced χ^2 = 80)

scattering	CN	R (Å)	σ^2 (Å^2)
Tc0 ⇆ I	6	2.67(3)	0.0010
Tc0 ⇆ Tc1	2	3.10(3)	0.0090

In order to increase the crystallinity of TcI_3 prepared at 150 °C, the compound was sealed in a tube and thermally treated at 150 °C for 5 days. After the reaction, no single crystals were obtained and the compound was characterized by PXRD, EDX spectroscopy, and SEM.

The sample exhibits a noticeable increase in crystallinity, and its PXRD pattern (Figure 5) is identical with the one obtained from the reaction at 300 °C; neither of the patterns was suitable enough for deriving detailed structural information.[19] The EDX spectra (Figure S5 in the SI) show Tc Lα and I Lα peaks, which indicate the material to be a binary technetium iodide; EDX quantification indicates that the compound has the stoichiometry $TcI_{3.1(3)}$.

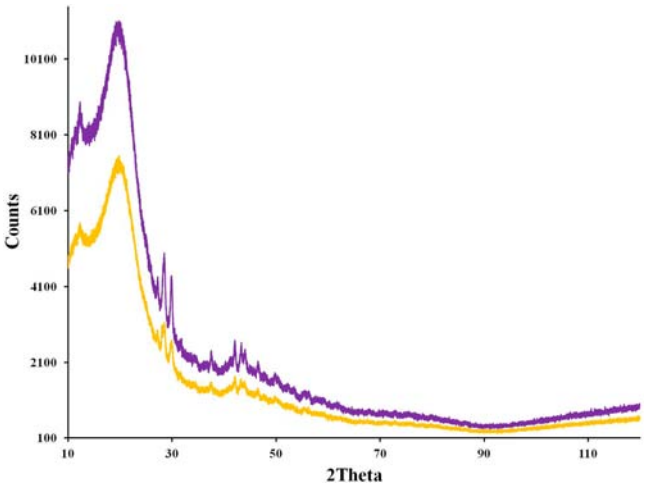

Figure 5. PXRD pattern of products from the reaction of $Tc_2(O_2CCH_3)_4Cl_2$ with HI(g) at 150 °C (purple) and 300 °C (orange) after sintering for 5 days at the respective temperatures.

SEM analysis shows TcI_3 to be composed of granulated clumps ranging from 10 to 100 μm in size. Within these clumps, single-crystal inclusions (~5 μm) with the stoichiometry TcI_3 are randomly dispersed (Figure 6).

The solid-state reaction of technetium metal with iodine (~1:4 Tc/I) was investigated in sealed Pyrex ampules in the temperature range 250−400 °C for 2 weeks. After those reactions, no single crystals were obtained, and the resulting powders were analyzed by PXRD. PXRD analysis indicates that technetium begins to react with iodine at 300 °C while higher yields of the product are obtained at 400 °C. After the reaction at 400 °C, the PXRD pattern of the product shows several new peaks (Figure 7) that match the ones of TcI_3 synthesized from $Tc_2(O_2CCH_3)_4Cl_2$ and HI(g); this indicates that TcI_3 is the primary product from the reaction of technetium metal and excess iodine.

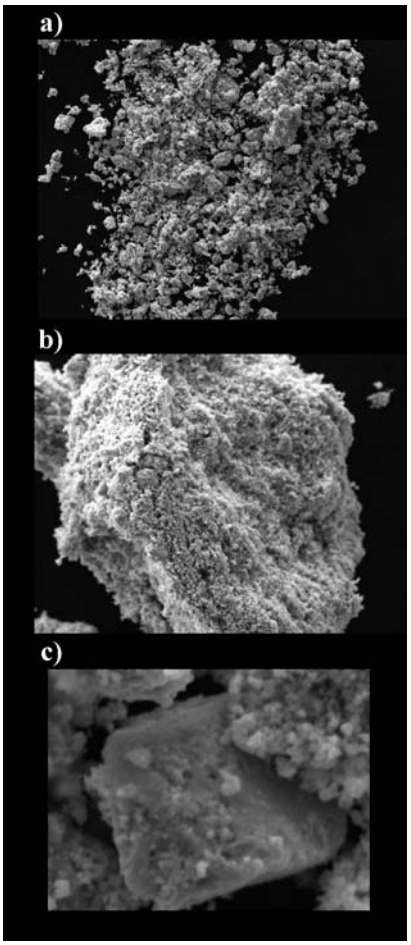

Figure 6. SEM images of TcI_3: (a) powder at 200× magnification; (b) individual piece of powder at 500× magnification; (c) crystalline inclusion of TcI_3 at 5000× magnification.

Thermal Stability. The thermal behavior of TcI_3 obtained from the reaction of $Tc_2(O_2CCH_3)_4Cl_2$ with flowing HI(g) at 150 °C was investigated in sealed Pyrex ampules under vacuum at 450 °C. The PXRD pattern indicates that the sample consists of technetium metal as a single phase.

DISCUSSION

Preparation. Molecular transition-metal acetate dimers are known for many second- and third-row metals: $M^{II}_2(O_2CCH_3)_4$ (M = Mo, W, Rh) and $M^{III}_2(O_2CCH_3)_4X_2$ (M = Re, Tc, Os). The reaction of these compounds (Mo, Rh, Re, and Tc) with flowing HX(g) at elevated temperatures is a direct route to binary metal halides (Table 2).[5] For molybdenum, these reactions yield the β-MoX_2 (X = Cl, Br, I) series, whereas for rhodium, these reactions result in the formation of RhX_3 and the metal. The same reactions with flowing HX(g) (X = Cl, Br, I) and $Re_2(O_2CCH_3)_4Cl_2$ yield Re_3X_9 containing the triangular Re_3^{9+} core with Re═Re bonds.[3,24,26]

For technetium, the predicted Tc_3Br_9 and Tc_3I_9 structures were not obtained via this synthetic route; this result contrasts with the one of the chlorine system that yields Tc_3Cl_9 with a

dx.doi.org/10.1021/ic402278c | Inorg. Chem. 2013, 52, 14309−14316

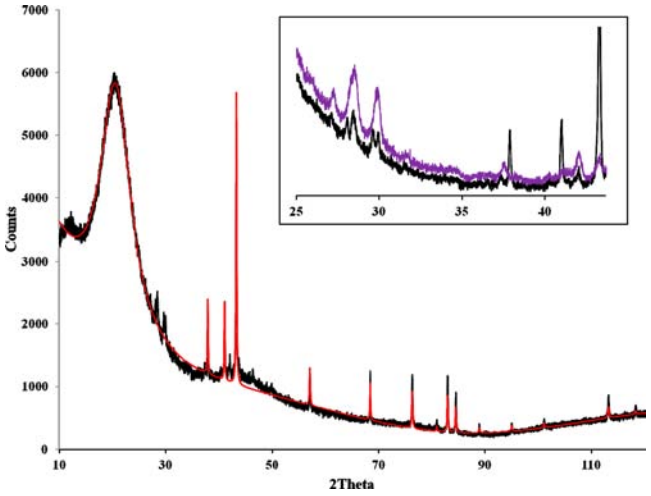

Figure 7. PXRD pattern of the products from the reaction of technetium metal and elemental iodine at 400 °C for 2 weeks (black) and fit with technetium metal (red). Inset: comparison of the product (black) to TcI_3 from the reaction of $Tc_2(O_2CCH_3)_4Cl_2$ with HI(g) (purple).

Table 2. Reactions of Metal−Metal-Bonded Acetate Compounds of Second- and Third-Row Transition Metals of Groups 6−8 with Flowing HX(g) (X = Cl, Br, I) at Various Temperatures and the Respective Products

reaction	150 °C/250 °C[a]	300 °C/340 °C[b]
$Tc_2(O_2CCH_3)_4Cl_2$ + HCl(g)[3]	$Tc_2(O_2CCH_3)_2Cl_4$	Tc_3Cl_9 (α-$TcCl_3$)
$Tc_2(O_2CCH_3)_4Cl_2$ + HBr(g)[c]	$TcBr_3$	$TcBr_3$
$Tc_2(O_2CCH_3)_4Cl_2$ + HI(g)[c]	TcI_3	TcI_3
$Re_2(O_2CCH_3)_4Cl_2$ + HX(g) (X = Cl, Br, I)[5,26]	$Re_2(O_2CCH_3)_2Cl_4$[a]	Re_3X_9 (X = Cl, Br, I)[b]
$Mo_2(O_2CCH_3)_4$ + HX(g) (X = Cl, Br, I)[5]	NR	β-MoX_2
$Os_2(O_2CCH_3)_4$ + HX(g)[d]	NR	NR

[a]Reaction occurs at 250 °C. [b]Reaction occurs at 340 °C. [c]Reported in this work. [d]NR: not reported.

Tc_3^{9+} core under similar conditions. In light of previous experiments that have demonstrated $TcBr_3$ as a starting material to phosphine complexes, this method for synthesizing weighable amounts of tribromide and triiodide will allow for the synthesis of other novel compounds.[27]

The reaction between technetium metal and iodide at 450 °C produces TcI_3; similar behavior is observed for molybdenum, tungsten, and ruthenium, all of which form triiodide species from analogous reactions (Table 3).[1b,28−32] For rhenium, no reaction between the metal and iodine in sealed tubes occurred in the temperature range 170−180 °C, which is also observed for technetium at lower reaction temperatures, i.e., 250 °C,[33] although for tungsten and ruthenium, both triiodides can be obtained from the reaction of the elements with iodine at elevated temperatures.[30−32] Osmium triiodide has been synthesized from decomposition of $(H_3O)_2OsI_6$ or the reaction of OsI_2 with iodine,[11a] but no data on the reaction of the osmium metal with elemental iodine were reported.

Structure. Technetium triiodide consists of face-sharing TcI_6 octahedra, structures that are also found for the ruthenium and molybdenum homologues. Five different structure types have been identified for the second- and third-row transition-metal triiodides spanning groups 4−10 (d^0−d^6).[34] These triiodides are comprised of either infinite chains or layered sheet structures (Figure 8). The "TiI_3" structure is the most common structure type found for d^1−d^5 transition-metal MX_3 phases (M = Zr, Hf, β-Nb, Mo, Tc, Ru, X = Br, I; M = Os, X = Br). The "TiI_3" structure type is composed of infinite chains of distorted face-sharing MX_6 octahedra (Figure 8a). The distortion within the chain occurs from alternating M−M distances and the correlative formation of M−M pairs, resulting in an "out-of-phase" displacement of the metal atoms and a structural deviation from hexagonal to orthorhombic symmetry.[34,35] Similar to the other NbX_3 phases (X = Cl, Br), α-NbI_3 takes the "$Nb_{3-x}Cl_8$" structure type (Figure 8b), which is a

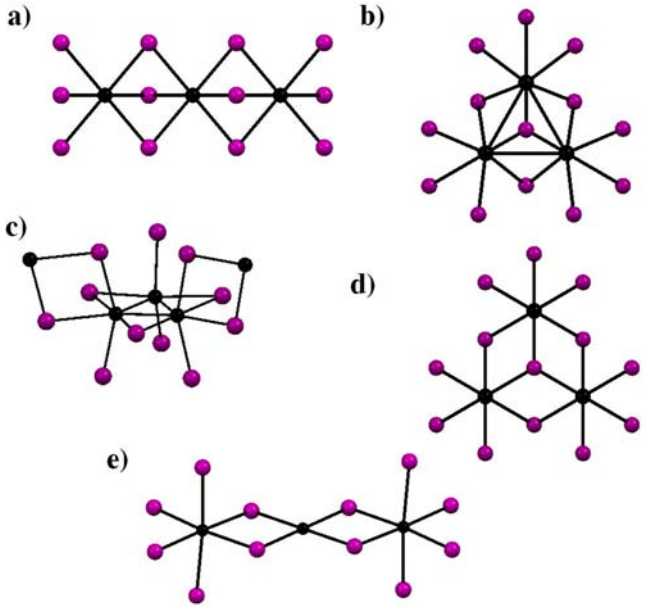

Figure 8. Ball-and-stick representations of second- and third-row transition-metal triiodide structure types: (a) zirconium, hafnium, β-niobium, molybdenum, technetium, ruthenium, and osmium; (b) niobium; (c) rhenium; (d) rhodium and iridium; (e) platinum. The metal atoms are in black, and the I atoms are in purple.

Table 3. Reactions of Second- and Third-Row Transition Metals of Groups 6−8 with Elemental Iodine

element	conditions	products
molybdenum	sealed-tube reaction at 500 °C[28,29]	MoI_3 and MoI_2
technetium	sealed-tube reaction at 300−400 °C[a]	TcI_3
ruthenium	sealed-tube reaction at 350 °C[30,31]	RuI_3
tungsten	sealed-tube reaction at 500 °C[32]	WI_3
rhenium	flowing iodine and sealed-tube reaction at 170−180 °C[33]	no reaction
osmium	NR[b]	

[a]This work. [b]Not reported.

dx.doi.org/10.1021/ic402278c | Inorg. Chem. 2013, 52, 14309−14316

homogeneous mixture of M_3X_8 and MX_4.[36] For rhenium, the Re_3X_9 motif is found for the chloride, bromide, and iodide (Figure 8c). This structural arrangement consists of a Re_3^{9+} triangular core with Re═Re double bonds, which for the bromide and iodide bridge from two adjacent Re atoms, unlike the chloride, which bridges all three atoms, forming layers of sheets.[24,26] Although the "$AlCl_3$" structure type (Figure 8d) is not predominately found for transition-metal tribromides or triiodides because of the large polarizability of bromine and iodine, both d^6 metals rhodium and iridium exhibit the "$AlCl_3$" structure type in their tribromides and triiodides; these are comprised of infinite layers of edge-sharing MX_6 octahedra (X = Br, I).[37,38] No triiodide has been characterized or reported for palladium; for platinum, the structure of PtI_3 is unique and consists of infinite chains of alternating PtI_6 octahedra and PtI_4 tetrahedra (Figure 8e).[39] WI_3 and TaI_3 have been prepared from the reaction of the respective metals and iodine, but their X-ray crystallographic structures have not been reported.[32,40]

Properties. Technetium tribromide is thermally unstable and decomposes to $Na\{[Tc_6Br_{12}]_2Br\}$ in a Pyrex sealed tube under vacuum at 450 °C.[12] Thermal decomposition performed in a quartz tube did not provide a crystalline product, which suggests that the source of the sodium in the compound originates from the Pyrex tube. It is still an open question whether $TcBr_2$ is accessible by thermal decomposition routes and whether its structure will be the "naked" Tc_6Br_{12} cluster or be similar to $TcCl_2$. Other MBr_3 (M = Mo, Re, Ru) are also susceptible to thermal decomposition. $MoBr_3$ disproportionates to Mo_6Br_{12} and $MoBr_4$ at 600 °C,[41] whereas for $ReBr_3$ and $RuBr_3$, both compounds decompose to the respective metals and Br_2 at temperatures above 450 °C.[42,43]

Technetium triiodide obtained from the reaction $Tc_2(O_2CCH_3)_4Cl_2$ with HI(g) at 150 and 300 °C is not hygroscopic, but it slowly releases iodine at room temperature. Technetium triiodide is insoluble in acetone, diethyl ether, dichloromethane, deionized H_2O, and 12 M HCl. An attempt to prepare TcI_2 from thermal decomposition of TcI_3 was unsuccessful; technetium triiodide is thermally unstable and decomposes to the metal at 450 °C under vacuum. Direct decomposition to technetium metal also suggests that no other TcI_{3-x} species are thermally stable and that the formation of TcI_3 is thermodynamically unfavorable at these temperatures. In comparison, MoI_3 decomposes to MoI_2 with the Mo_6I_{12} structural motif at 100 °C,[44] while ReI_3 decomposes stepwise to the di- and monoiodides between 320−420 and 420−470 °C, respectively, and the metal and iodine at temperatures above 580 °C.[45]

CONCLUSION

Technetium triiodide, the first technetium binary iodide to be reported, was obtained in the solid state from the reaction of $Tc_2(O_2CCH_3)_4Cl_2$ with HI(g) at 150 and 300 °C and from the reaction of technetium metal and iodine in a sealed tube at 400 °C. Technetium triiodide was characterized by spectroscopic, diffraction, and microscopic techniques; EXAFS results indicate the compound to consist of face-sharing TcI_6 octahedra. The reactions of $Tc_2(O_2CCH_3)_4Cl_2$ with HBr(g) at 150 and 300 °C $TcBr_3$ with the TiI_3 structure type consisting of face-sharing $TcBr_6$ octahedra. The behavior of $Tc_2(O_2CCH_3)_4Cl_2$ with HX(g) (X = Br, I) does not follow the one under HCl(g), and Tc_3X_9 (X = Br, I) are not obtained. Both $TcBr_3$ and TcI_3 consist of face-sharing TcX_6 octahedra; this structure is also found for other MX_3 (M = Ru, Mo; X = Br, I); this indicates that the heavier halide chemistry of Tc^{III} is more similar to that of Mo^{III} and Ru^{III} and not to Re^{III}, the latter exhibiting the triangular Re_3X_9 clusters in their structure.

The thermal behavior of $TcBr_3$ and TcI_3 was investigated under vacuum in sealed ampules at 450 °C. Both compounds are unstable, $TcBr_3$ decomposes to $Na\{[Tc_6Br_{12}]_2Br\}$ and technetium metal in a Pyrex tube and to technetium metal in a quartz tube. Technetium triiodide decomposes to technetium metal, and no divalent phases were observed. Technetium triiodide is insoluble in water and organic solvents. The thermal and solubility properties of TcI_3 might be of particular interest for nuclear fuel cycle applications (i.e., Mo/Tc separation using halide volatility processes and the development of Tc−I waste forms).

Previous calculations indicate that Tc_3Br_9 and Tc_3I_9 should be stable; our results show that that these are not observed in the temperature range 150−400 °C and that the known TcX_3 (X = Br, I) phases decompose to technetium metal above 450 °C. This suggests that low-temperature routes would be required for the preparation of Tc_3X_9 (X = Br, I): such routes might include metathesis reactions using α-$TcCl_3$ as a precursor or thermal decomposition of Ag_2TcX_6 under vacuum below 150 °C.[46]

ASSOCIATED CONTENT

Supporting Information

SEM and EDX spectra of $TcBr_3$ and TcI_3, additional PXRD figures and tables, IR spectra, and EXAFS data. This material is available free of charge via the Internet at http://pubs.acs.org.

AUTHOR INFORMATION

Corresponding Author

*E-mail: erikvjohnstone@gmail.com.

Notes

The authors declare no competing financial interest.

ACKNOWLEDGMENTS

Funding for this research was provided by NEUP grant "Development of Alternative Technetium Waste Forms" from the U.S. Department of Energy, Office of Nuclear Energy, through INL/BEA, LLC (Grant 89445). Use of the Advanced Photon Source (APS) at Argonne was supported by the U.S. Department of Energy, Office of Science, Office of Basic Energy Sciences, under Contract DE-AC02-06CH11357. The authors thank Trevor Low and Julie Bertoia for exceptional health physics support, Dr. Minghua Ren for significant support with SEM and EDX, and Dr. Sungsik Lee at the APS for outstanding support during EXAFS experiments.

DEDICATION

This manuscript is dedicated to Dr. Frank Kinard, a gifted teacher and friend who inspired so many.

REFERENCES

(1) (a) Schwochau, K. *Technetium: Chemistry and Radiopharmaceutical Applications*; Wiley-VCH: Weinheim, Germany, 2000. (b) Canterford, J. H.; Colton, R. *Halides of the Second and Third Row Transition Metals*; John Wiley and Sons: New York, 1968. (c) Poineau, F.; Mausolf, E.; Jarvinen, G. D.; Sattelberger, A. P.; Czerwinski, K. R. *Inorg. Chem.* **2013**, *52* (7), 3573−3578. (d) Sattelberger, A. P. *In Multiple Bonds between Metal Atoms*, 3rd ed.; Cotton, F. A., Murillo, C. A., Walton, R. A., Eds.; Springer: New York, 2005; Chapter 7.

(2) Poineau, F.; Rodriguez, E. E.; Forster, P. M.; Sattelberger, A. P.; Cheetham, A. K.; Czerwinski, K. R. *J. Am. Chem. Soc.* **2009**, *131* (3), 910−911. (b) Poineau, F.; Malliakas, C. D.; Weck, P. F.; Scott, B. L.; Johnstone, E. V.; Forster, P. M.; Kim, E.; Kanatzidis, M. G.; Czerwinski, K. R.; Sattelberger, A. P. *J. Am. Chem. Soc.* **2011**, *133*, 8814−8817.
(3) Poineau, F.; Johnstone, E. V.; Weck, P. F.; Kim, E.; Forster, P. M.; Scott, B. L.; Sattelberger, A. P.; Czerwinski, K. R. *J. Am. Chem. Soc.* **2010**, *132* (45), 15864−15865.
(4) Poineau, F.; Johnstone, E. V.; Weck, P. F.; Forster, P. M.; Kim, E.; Czerwinski, K. R.; Sattelberger, A. P. *Inorg. Chem.* **2012**, *51* (9), 4915−4917.
(5) (a) Glicksman, H. D.; Hamer, A. D.; Smith, T. J.; Walton, R. A. *Inorg. Chem.* **1976**, *15* (9), 2205−2209. (b) Glicksman, H. D.; Walton, R. A. *Inorg. Chem.* **1978**, *17* (1), 200−201. (c) Santure, D. J.; Huffman, J. C.; Sattelberger, A. P. *Inorg. Chem.* **1985**, *24* (3), 371−378.
(6) Johnstone, E. V.; Poineau, F.; Forster, P. M.; Ma, L.; Hartmann, T.; Cornelius, A.; Antonio, D.; Sattelberger, A. P.; Czerwinski, K. R. *Inorg. Chem.* **2012**, *51* (15), 8462−8467.
(7) (a) Weck, P. F.; Sergeeva, A. P.; Kim, E.; Boldyrev, A. I.; Czerwinski, K. R. *Inorg. Chem.* **2011**, *50* (3), 1039−1046. (b) Aslanov, L. A.; Volkov, S. V.; Kolesnichenko, V. L.; Rybakov, V. B.; Timoshchenko, N. I. *Ukr. Khim. Zh.* **1992**, *58* (4), 279−281.
(8) Miroslavov, A. E.; Borisova, I. V.; Sidorenko, G. V.; Suglobov, D. N. *Radiokhimiya* **1991**, *33* (6), 14−19.
(9) Cotton, F. A.; Wilkinson, G.; Murillo, C. A.; Bochmann, M. *Advanced Inorganic Chemistry*, 6th ed.; John Wiley and Sons: New York, 1999.
(10) Prussin, S. G.; Olander, D. R.; Lau, W. K.; Hansson, L. *J. Nucl. Mater.* **1988**, *154* (1), 25−37.
(11) (a) Fergusson, J. E.; Robinson, B. H.; Roper, W. R. *J. Chem. Soc.* **1962**, 2113−2115. (b) Degner, M.; Holle, B.; Kamm, J.; Pilbrow, M. F.; Thiele, G.; Wagner, D.; Weigl, W.; Wodtisch, P. *Transition Met. Chem.* **1976**, *1*, 41−47.
(12) Johnstone, E. V.; Grant, D. J.; Poineau, F.; Fox, L.; Forster, P. M.; Ma, L.; Gagliardi, L.; Czerwinski, K. R.; Sattelberger, A. P. *Inorg. Chem.* **2013**, *52* (10), 5660−5662.
(13) Poineau, F.; Sattelberger, A. P.; Czerwinski, K. R. *J. Coord. Chem.* **2008**, *61* (15), 2356−2370.
(14) The gold foil was used to prevent any reaction between the quartz/Pyrex reaction vessels and formed product. Corbett, J. D. *Inorg. Synth.* **1983**, *22*, 13.
(15) Sheldrick, G. M. *Acta Crystallogr., Sect. A* **2008**, *64*, 112.
(16) Ressler, T. *J. Synchrotron Radiat.* **1998**, *5*, 118−122.
(17) Rehr, J. J.; Albers, R. C. *Rev. Mod. Phys.* **2000**, *72*, 621−654.
(18) Ravel, B. *J. Synchrotron Radiat.* **2001**, *8*, 314−316.
(19) 2θ and *d*-spacing coordinates are presented in the S in Table S1.
(20) Almahamid, I.; Bryan, J. C.; Bucher, J. J.; Burrell, A. K.; Edelstein, N. M.; Hudson, E. A.; Kaltsoyannis, N.; Lukens, W. W.; Shuh, D. K.; Nitsche, H.; Reich, T. *Inorg. Chem.* **1995**, *34*, 193−198.
(21) Poineau, F.; Sattelberger, A. P.; Conradson, S. D.; Czerwinski, K. R. *Inorg. Chem.* **2008**, *47*, 1991−1999.
(22) Poineau, F.; Johnstone, E. V.; Forster, P. M.; Ma, L.; Sattelberger, A. P.; Czerwinski, K. R. *Inorg. Chem.* **2012**, *51*, 9563−9570.
(23) Poineau, F.; Johnstone, E. V.; Sattelberger, A. P.; Czerwinski, K. R. *J. Radioanal. Nucl. Chem.* **2013**, DOI: 10.1007/s10967-013-2743-0.
(24) Bennett, M. J.; Cotton, F. A.; Foxman, B. M. *Inorg. Chem.* **1968**, *7*, 1563−1569.
(25) The separation (*d*) between the center of two face-sharing regular octahedra (with *a* = distance from center to vertices) is given by the formula $d = 2a\sqrt{3}/3$. When this formula is transposed to TcI_6 octahedra (*a* = Tc−I and *d* = Tc−Tc), the Tc−Tc separation between two face-sharing TcI_6 octahdra (Tc−I = 2.67 Å) is calculated to be 3.08 Å.
(26) Cotton, F. A.; Mauge, J. T. *Inorg. Chem.* **1964**, *3* (10), 1402−1407.
(27) Poineau, F.; Weck, P. F.; Forster, P. M.; Sattelberger, A. P.; Czerwinski, K. R. *Dalton Trans.* **2009**, *46*, 10338−10342.
(28) Lewis, J.; Machin, D. J.; Nyholm, R. S.; Pauling, P.; Smith, P. W. *Chem. Ind.* **1960**, 259−260.
(29) Sato, T.; Fukui, H.; Sasaki, H.; Tachikawa, T. *Denki Kagaku* **1988**, *56* (10), 860−863.
(30) Schnering, H. G.; Brodersen, K.; Moers, F.; Breitbach, H. K.; Thiele, G. *J. Less-Common Met.* **1966**, *11*, 288−289.
(31) Breitbach, H. K. Graduate thesis, received 1965.
(32) Schaefer, H.; Schulz, H. G. *Z. Anorg. Allg. Chem.* **1984**, *516*, 196−200.
(33) Rulfs, C. L.; Elving, P. J. *J. Am. Chem. Soc.* **1957**, *72*, 3304.
(34) Lin, J.; Miller, G. *Inorg. Chem.* **1993**, *32*, 1476−1487.
(35) (a) Merlino, S.; Labella, L.; Marchetti, F.; Toscani, S. *Chem. Mater.* **2004**, *16*, 3895−3903. (b) Hillebrecht, H.; Ludwig, Th.; Thiele, G. *Z. Anorg. Allg. Chem.* **2004**, *630*, 2199−2204. (c) Lachgar, A.; Dudis, D. S.; Corbett, J. D. *Inorg. Chem.* **1990**, *29*, 2242−2246.
(36) Simon, A.; von Schnering, H. G. *J. Less-Common Met.* **1966**, *11*, 31−46.
(37) (a) Hillebrecht, H.; Schmidt, P. J.; Rotter, H. W.; Thiele, G.; Zoennchen, P.; Bengel, H.; Cantow, H. J.; Magonov, S. N.; Whangbo, M. H. *J. Alloys Compd.* **1997**, *246*, 70. (b) Schaefer, H.; Schnering, H. G.; Tillack, J.; Kuhnen, F.; Woehrle, H.; Baumann, H. *Z. Anorg. Allg. Chem.* **1967**, *353*, 281−310.
(38) (a) Hulliger, F. *Structural Chemistry of Layer-Type Phases*; D. Reidel Publishing Co.: Dordrecht, The Netherlands, 1976; p 164. (b) Babel, D.; Deigner, P. *Z. Anorg. Allg. Chem.* **1965**, *339*, 57.
(39) Thiele, G.; Steiert, D.; Wagner, D.; Wochner, H. *Z. Anorg. Allg. Chem.* **1984**, 207−213.
(40) Chizhikov, D. M.; Rabinovich, B. N. *Dokl. Akad. Nauk SSR* **1960**, *134*, 368−370.
(41) Schaefer, H. *Anorg. Allg. Chem.* **1986**, *534*, 206−208.
(42) Kolbin, N. I.; Ovchinnikov, K. V. *Zh. Neorg. Khim.* **1968**, *13* (8), 2306−2307.
(43) Shchukarev, S. A.; Kolvin, N. I.; Ryabov, A. N. *Vestn. Leningr. Univ.* **1961**, *16*, 100−104.
(44) Klanberg, F.; Koholschutter, H. W. *Z. Naturforsch.* **1960**, *15b*, 616.
(45) (a) Drobot, D. V.; Mikhailova, L. G. *Zh. Neorg. Khim.* **1973**, *18* (1), 31−34. (b) Drobot, D. V.; Mikhailova, L. G.; Sushchev, A. V. *Zh. Neorg. Khim.* **1976**, *21* (12), 3348−3354.
(46) Fergusson, J. E.; Hickford, J. H. *Aust. J. Chem.* **1970**, *23* (3), 453−461.